Turkish Journal of Electrical Engineering & Computer Sciences

http://journals.tubitak.gov.tr/elektrik/

Research Article

Turk J Elec Eng & Comp Sci
(2014) 22: 957 – 969

doi:10.3906/elk-1211-161

# Performance evaluation of the wave atom algorithm to classify mammographic images

**Nebi GEDİK**[1,*], **Ayten ATASOY**[2]

[1]Department of Maritime Transportation and Management Engineering, Faculty of Marine Sciences, Karadeniz Technical University, Sürmene, Trabzon, Turkey

[2]Department of Electrical and Electronics Engineering, Faculty of Engineering, Karadeniz Technical University, Trabzon, Turkey

**Received:** 28.11.2012 • **Accepted:** 14.01.2013 • **Published Online:** 17.06.2014 • **Printed:** 16.07.2014

**Abstract:** The most common type of cancer seen in women is breast cancer. To enable recovery from this severe disease, monitoring and early detection must be provided, and related precautions must be taken as a first step. During diagnosis, some cases may be overlooked due to fatigue and eyestrain, because the determination of abnormalities is a repetitive procedure. In this study, a computer-aided diagnosis (CAD) system, using the wave atom transform (WAT) algorithm and support vector machine (SVM), is proposed to evaluate mammography images. During the process, the region of interest (ROI) is defined before applying the method. The system includes a feature extraction approach based on the WAT algorithm. In terms of classification, the process has 2 main stages: the classification of normal/abnormal regions and malignant/benign ones. The proposed system also uses principle component analysis (PCA) for further dimensional reduction and feature selection. A dataset from the Mammographic Image Analysis Society database is employed for testing and measuring the performance of the proposed system. The best success rates in this work are obtained using the coefficients at scales of 1, 2, and 3, by employing SVM with PCA. The maximum classification success rate to define the regions of interest as normal/abnormal is 100%. The success rate of malignant/benign classification is also achieved as 100% in the tests. According to the results, it is observed that these features ensure important support for more comprehensive clinical investigations and the results are very encouraging when mammograms are categorized via WAT, PCA, and SVM.

**Key words:** Mammography, CAD system, wave atom transform, SVM, ROC analysis

## 1. Introduction

Breast cancer is one of the most dangerous types of cancer for women worldwide. More than 11% of women suffer from this type of cancer during their lifetime. The estimations of The World Health Organization's International Agency for Research on Cancer (IARC) predict that more than 1 million women worldwide will be infected by breast cancer yearly, and more than 400,000 will die each year [1]. The most important aspect in the treatment of breast cancer is early detection [2]. On the other hand, early detection is not an easy task and biopsy is used to obtain the most accurate results in diagnosis. However, a biopsy operation is very costly and can be difficult for the patients.

Mammography is the best available inspection facility to detect breast cancer and it can disclose a signif-

*Correspondence: ngedik@ktu.edu.tr

icant demonstration of abnormality, such as masses, microcalcifications, bilateral asymmetry, and architectural distortion [3]. Mammography, a special X-ray imaging technique, is used to take exhaustive pictures of the breasts. Low-dose X-ray, high-contrast, and high-resolution film are used for mammography, and its X-ray part was planned particularly to scan the breasts [3].

Among the hundreds of images examined by a radiologist, only a few images contain cancer. The determination of abnormalities is a successive procedure. It leads to several physical drawbacks in the human body, such as fatigue and eye strain; thus, some abnormalities may be overlooked. Therefore, computer-aided diagnosis (CAD) systems have been developed to assist radiologists in the determination of abnormalities using mammography that may point out the existence of abnormality. CAD systems work only as a second reader, and the definite diagnosis and last decision about the case is always left to the radiologist. These automated systems have improved radiologists' ability to achieve the best accuracy on breast cancer detection [4]. In this case, many studies have been done using different algorithms in the literature including CAD systems [5–9]. Wang et al. [10] proposed an algorithm based on independent component analysis (ICA) and least squares (LS)-support vector machine (SVM). They selected variables using the theory of statistics. Next, the ICA was applied to these selected variables for extracting the ICA components. Finally, LS-SVM was used to classify the data. Their experimental results showed that the ICA and LS-SVM method was better than the solely applied LS-SVM method. Polat and Güneş [11] used the LS-SVM classifier algorithm for breast cancer diagnosis. They achieved classification accuracies of 95.89%, 96.59%, and 97.08% for training/testing partitions of 50%–50%, 70%–30% and 80%–20%, respectively.

The extraction of features from an image is a significant stage in image processing and CAD systems. Features can be obtained from spatial data or data on a different space. Different space modalities that use a transform, such as Fourier, wavelet, ridgelet, contourlet, or curvelet, can be beneficial to distinguish a specific item of data. Multiresolution tools allow conservation of an image with respect to a specific resolution. They also provide zooming into the image. Multiresolution analyses are widely used in image processing applications [12,13]. In this direction, a few algorithms have been improved to extract features in mammographic images using wavelet. Rajkumar et al. [14] presented a comparative study that used 2 different wavelets for the classification of mammographic images to detect tumors. A small part of the biggest coefficients from discrete wavelet transform (DWT) and stationary wavelet transform (SWT) were used as features. In their paper, mammographic images were classified as normal, benign, and malignant. The success rate of the classification obtained from DWT was 83% and 76% from SWT. They also compared Euclidean and Bray Curtis distances for appropriate classification.

Boccignone et al. [15] proposed a CAD system using wavelet transform to detect microcalcifications on mammograms. They decomposed each image into different resolution levels and implemented a thresholding technique to separate the microcalcifications. In the thresholding stage, Renyi entropy was utilized. Classification was carried out using wavelet coefficients without inverse wavelet transform. Gurcan et al. [16] presented a method based on a 'subband' decomposition filter bank, which used nonlinear filters to classify microcalcifications. They decomposed each mammogram into subimages using the filter bank. The detail-image was divided into overlapping square regions and then the skewness and kurtosis were computed. A region that had high positive skewness and kurtosis was marked as a ROI. To find the microcalcification locations, they used an outlier labeling method and obtained an enhanced mammogram by emphasizing the microcalcification locations. They compared linear and nonlinear subband decomposition structures and found that both structures were successfully identified microcalcification regions. Gurcan et al. [17] used the subband domain to detect microcalcification clusters. The mammograms were processed by a subband decomposition filterbank. The resulting bandpass subimages were analyzed to detect microcalcifications. Skewness and kurtosis were used to find the locations of microcalcification clusters. High positive skewness and kurtosis indicated the microcalcification areas. Their experimental studies showed that the method was successful to detect microcalcifications regions. Bagci et al. [18] developed methods for the detection of microcalcification based on higher-order statistics (HOSs), and wavelet analysis. They divided each mammogram image into overlapping small windows. After that, a HOS was estimated in each window. Windows with HOS values higher than a threshold value were marked as regions containing microcalcification.

Moayedi et al. [19] presented a method to classify masses via contourlet and SVM. They used statistical features obtained from contourlet coefficients at the fourth decomposition, cooccurrence matrix, and geometrical features for each image. Moreover, they used a genetic algorithm to select features and a neural network classifier to classify them. Thus, they emphasized that the contourlet transform offers an improvement for the classification stage. Candes et al. [20] developed a curvelet transform to provide a powerful representation of objects with discontinuities throughout curves. It is very important to detect and to enhance the boundaries between different structures in medical images. Several studies have been done using curvelet transforms. Ali et al. [21] offered a curvelet transform modality for the fusion of computed tomography and magnetic resonance images. The curvelet transform provided successful results in their fusion experimentation. Bind et al. [22] presented a method based on a curvelet transform to detect objects in speckle images. They also built a segmentation method that provided a sparse expansion for a smooth image. Eltoukhy et al. [23] presented a comparative study including wavelet and curvelet transforms. The biggest 100 coef?cients, coming from each scale belonging to the wavelet and curvelet, were used to create a feature matrix for the classi?cation stage. They used a Euclidean distance classifier for the classification, and 142 mammogram images obtained from the Mammographic Image Analysis Society (MIAS) dataset were employed for training and testing of the system.

Eltoukhy et al. [24] introduced a method to classify mammographic images based on a curvelet transform. The developed method decomposes each image into different scales and angles. Here, different ratios from the biggest coefficients were selected for use as the feature vector and a different decomposition level was used to detect the scale that provides the maximum classification accuracy. The maximum success rate was obtained as 98.59% for normal and abnormal classification at a scale of 2 using 40% of the coefficients, and at a scale 3 using 40% and 70% of the coefficients. The conducted comparative study with a wavelet showed that features based on the curvelet yield a greater classification success rate than features based on the wavelet. Eltoukhy et al. [25] presented another method for breast cancer diagnosis. They developed a feature extraction technique based on the statistical t-test algorithm. The method builds a matrix that is created from coefficients' vectors of wavelet or curvelet transformation. After that, a dynamic threshold is implemented to get the most important features. The dataset is divided into 2 parts, called training and testing. For the classification stage, the SVM technique is used as a classifier. The dataset is classified as normal/abnormal and benign/malignant. The technique is repeated until the classification success rate increases to the highest value with the least coefficients.

In this study, we first isolate the ROI manually from mammographic images, and then each ROI is decomposed using wave atom transform (WAT) (at scales of 1, 2, 3, and 4), separately. To the best of our knowledge, there is no previous work using WAT to classify mammograms. Therefore, the objectives of this paper are to investigate the implementation of WAT on mammographic images and to also fill a gap in the literature. In this paper, we build the feature vector and the feature matrix using wave atom coefficients. First, we obtain wave atom coefficients for each scale. These coefficients are used to categorize the mammograms into normal or abnormal and benign or malignant. We then employ the SVM algorithm to classify the mammogram images. In our experiments, parameters $\sigma$ and $C$, which belong to the SVM, are selected to be 9 and 1000, respectively.

The rest of the paper is constructed as follows. Section 2 gives a brief introduction to the WAT. The experimental works and dataset obtained from the MIAS are described in detail in section 3. The results and conclusions are presented in sections 4 and 5, respectively.

## 2. WAT

WAT was presented by Demanet in 2007 [26]. The transformation, obeying the parabolic scaling law, can be considered a variant of 2-dimensional (2D) wavelet packets. WAT has 2 very significant properties. The first is the ability to adapt to arbitrary local directions of a pattern and the second is the ability to sparsely represent anisotropic patterns aligned with the axes. Wave atoms offer sharper frequency localization than other wave packets. It also has significant sparse expansion for oscillatory functions when compared with wavelets, curvelets, and Gabor atoms.

The forms of wave packets, known as wavelets, Gabor, ridgelets, curvelets, and wave atoms, are created using 2 parameters, which are $\alpha$ and $\beta$. These variables symbolize the decomposition and directional ability for all wave forms. The $\alpha$ and $\beta$ values are 1/2 for wave atoms and Figure 1 shows wave packet's support in the space and in frequency planes. Here, $\alpha$ corresponds to the multiscale structure of the transform and $\beta$ corresponds to directional selectivity.

Actually, wave atoms are built from the tensor products of 1D wave packets. One-dimensional (1D) wave packets can be represented as $\psi^j_{m,n}(x)$, where $j,m \geq 0$ and $n \in Z$. The frequency restrictions are $\pm\omega_{j,m} = \pm\pi 2^j m$ with $C_1 2^j \leq m \leq C_2 2^j$. The space restriction is defined as $x_{j,n}$=$2^j n$. The basic function can be written as follows:

$$\psi^j_{m,n}(x) = \psi^j_m\left(x - 2^j n\right) = 2^{j/2}\psi^0_m\left(2^j x - n\right). \tag{1}$$

Here, 2D wave atoms $\varphi_\mu(x_1 x_2)$ are constructed with subscript $\mu = (j, m, n)$, where $m = (m_1, m_2)$, $n = (n_1, n_2)$. Modifying Eq. (1), a 2D orthonormal basis is written as follows:

$$\varphi^+_\mu(x_1,x_2) = \psi^j_{m1}\left(x_1 - 2^{-j} n_1\right)\psi^j_{m2}\left(x_2 - 2^{-j} n_2\right), \tag{2}$$

$$\varphi^-_\mu(x_1,x_2) = H\psi^j_{m1}\left(x_1 - 2^{-j} n_1\right) H\psi^j_{m2}\left(x_2 - 2^{-j} n_2\right), \tag{3}$$

where H is a Hilbert transform. The wave atom tight frame is formed by a combination of Eqs. (2) and (3).

$$\varphi^{(1)}_\mu = \frac{\varphi^+_\mu + \varphi^-_\mu}{2}, \quad \varphi^{(2)}_\mu = \frac{\varphi^+_\mu - \varphi^-_\mu}{2}. \tag{4}$$

More details about WAT can be found in [26].

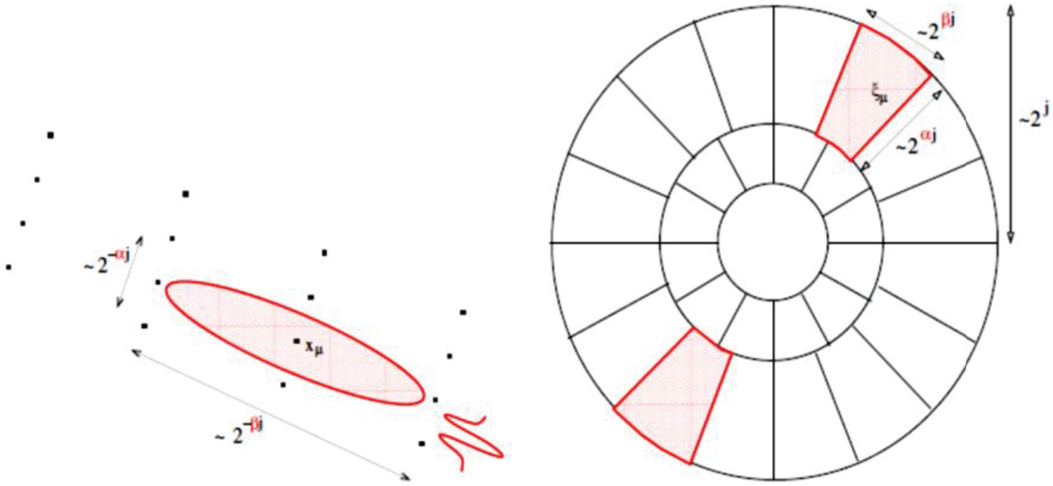


**Figure 1.** Wave atoms tiling in the space and frequency domains. This illustrates the essential support of a wave packet with parameters $(\alpha, \beta)$, in space (left), and in frequency (right).

## 3. Details of the experimental work

In this paper, a multiresolution representation of the mammographic images is realized using WAT. Mammographic images are cropped manually and subimages (ROIs) are generated. ROIs contain many abnormalities, called microcalcification, circumscribed mass, ill-defined mass, speculated mass, architectural distortion, and asymmetry. For feature extraction, WAT at scales of 1, 2, 3, and 4 is applied to each ROI to obtain the feature vector. The classification process is performed using SVM.

In this paper, a dataset supplied by the MIAS [27] is used to implement the wave atom algorithm. In the MIAS database, images have been examined and labeled by expert radiologists. The datasets are widely used in mammographic research [25] in various cases. This database contains a file description list belonging to the mammograms and provides appropriate details about each image. Some of these details are the class of abnormality, (x,y) coordinates of the abnormality according to its center, and approximate radius of a circle surrounding the abnormality. Such details are required because the dataset includes various cases. The database is publicly available for scientific research.

In this study, 200 mammogram images, including 50 malignant, 50 benign, and 100 normal, are used to test the system and utilize the largest dataset in the literature [8]. ROIs containing the abnormalities are manually cropped for each mammogram. ROIs are found according to (x,y) coordinates, showing the center of the abnormality, where the coordinates are given in the file list of the MIAS database. Mammographic images include unwanted parts, such as the pectoral muscle and label. These parts are eliminated by applying a cropping operation. The cropping operation is carried out adhering to the given coordinates. Thus, training and testing sets are created by cropping at a size of 128 $\times$ 128 pixels. An example of cropping and the fallow cards of the proposed diagnosis system are given in Figure 2.

In order to determine which scale gives a better result, the WAT is applied at scales of 1, 2, 3, and 4 after the mammograms are cropped as described above. The feature matrix is obtained from the feature vectors belonging to wave atom coefficients. In the classification stage, SVMs are applied to the training and testing datasets.

Three different methods have been applied for the evaluation of breast cancer diagnosis. These methods are classification accuracy, sensitivity, and specificity analysis and receiver operating characteristic (ROC) curves. The following expressions are used for the sensitivity and specificity analysis:

$$Sensitivity = \frac{TP}{TP\ +\ FN}(\%), \tag{5}$$

$$Specificity\ = \frac{TN}{FP\ +\ TN}(\%), \tag{6}$$

where TP, TN, FP, and FN indicate true positives, true negatives, false positives, and false negatives, respectively.

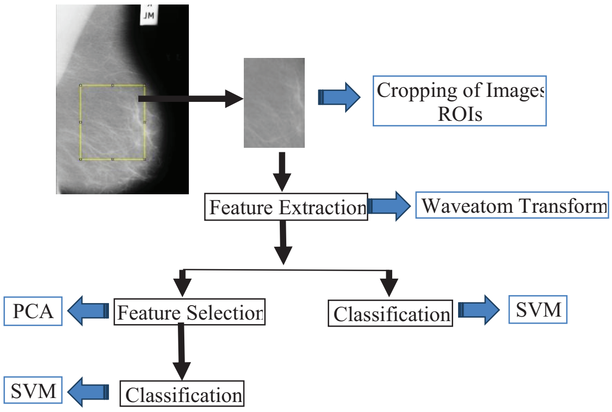


**Figure 2.** The system proposed for breast cancer diagnosis. First, the images are cropped, and WAT is then applied to the ROIs. The obtained features are classified both directly and using feature extraction.

## 4. Results and discussion

In the first step of this work, the dataset is classified as normal and abnormal using SVM algorithms. In this stage, the dataset is divided into 2 groups, as training and testing. Thus, the dataset is partitioned into 2 different groups of samples in terms of the ROI. Those samples include 100 normal and 100 abnormal mammogram images. Table 1 shows the success rates of the SVM method for the classification of images as normal and abnormal. After that, the second step of this work is the classification of images as malignant and benign types of abnormal mammograms. For this, 100 abnormal images from the MIAS database, which include 50 malignant and 50 benign, are used. The dataset is divided into 2 groups for training and testing, to examine the classification accuracy of the SVM. Thus, the dataset is partitioned into 2 different samples. The success rates of the SVM algorithms for the classification of mammogram images as malignant and benign are shown in Table 2. Figures 2 and 3 illustrate the ROC curves to show the effectiveness of each classifier using WAT. Figure 3 shows ROC curves for separation of images as normal and abnormal, and Figure 4 shows the ROC curves for malignant and benign types of images.

In this paper, an additional study for the classification of mammograms via WAT is performed using the principle component analysis (PCA) method for feature selection and dimensional reduction. Tables 3 and 4 show the success rates of SVM in the classifications of mammogram images, first as normal/abnormal, and second as malignant/benign, after applying PCA, respectively. In Table 4, it is observed that 100% classification accuracy is provided with wave atom coefficients at a scale of 1. Therefore, the feature selection process with PCA is not performed for malignant/benign classification.

The ROC curves for normal/abnormal separating with PCA at each scale are shown in Figure 5. Similarly, the ROC curves of the SVM classifier and PCA at each scale are shown in Figure 6 for the malignant/benign separating system.

**Table 1.** Success rates of the SVM algorithm in the classification of mammogram images as normal and abnormal.

| | Wave atom | | | |
|---|---|---|---|---|
| Scale | Accuracy (%) | Sensitivity | Specificity | Classifier |
| **1** | 94 | 0.89 | 1 | SVM |
| **2** | 69 | 0.38 | 1 | SVM |
| **3** | 55 | 0.10 | 1 | SVM |
| **4** | 53 | 0.06 | 1 | SVM |

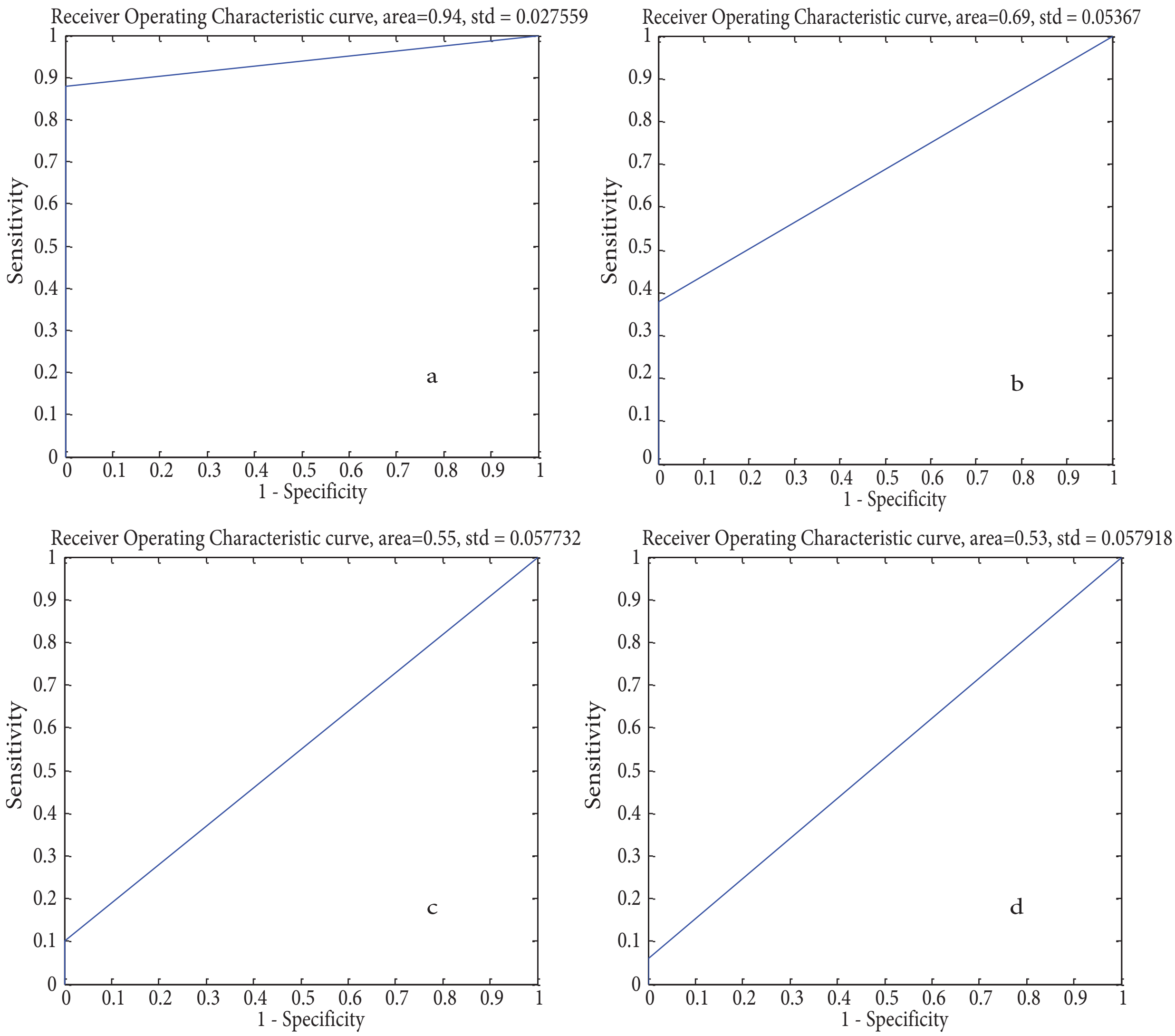


**Figure 3.** ROC curves for normal and abnormal classification with wave atom coefficients. According to the values of sensitivity and specificity: a) for a scale of 1, b) for a scale of 2, c) for a scale of 3, and d) for a scale of 4.

**Table 2.** Success rates of the SVM algorithm in the classification of mammogram images as malignant and benign.

| | Wave atom | | | |
|---|---|---|---|---|
| Scale | Accuracy (%) | Sensitivity | Specificity | Classifier |
| **1** | 100 | 1 | 1 | SVM |
| **2** | 62 | 1 | 0.24 | SVM |
| **3** | 56 | 1 | 0.12 | SVM |
| **4** | 54 | 1 | 0.08 | SVM |

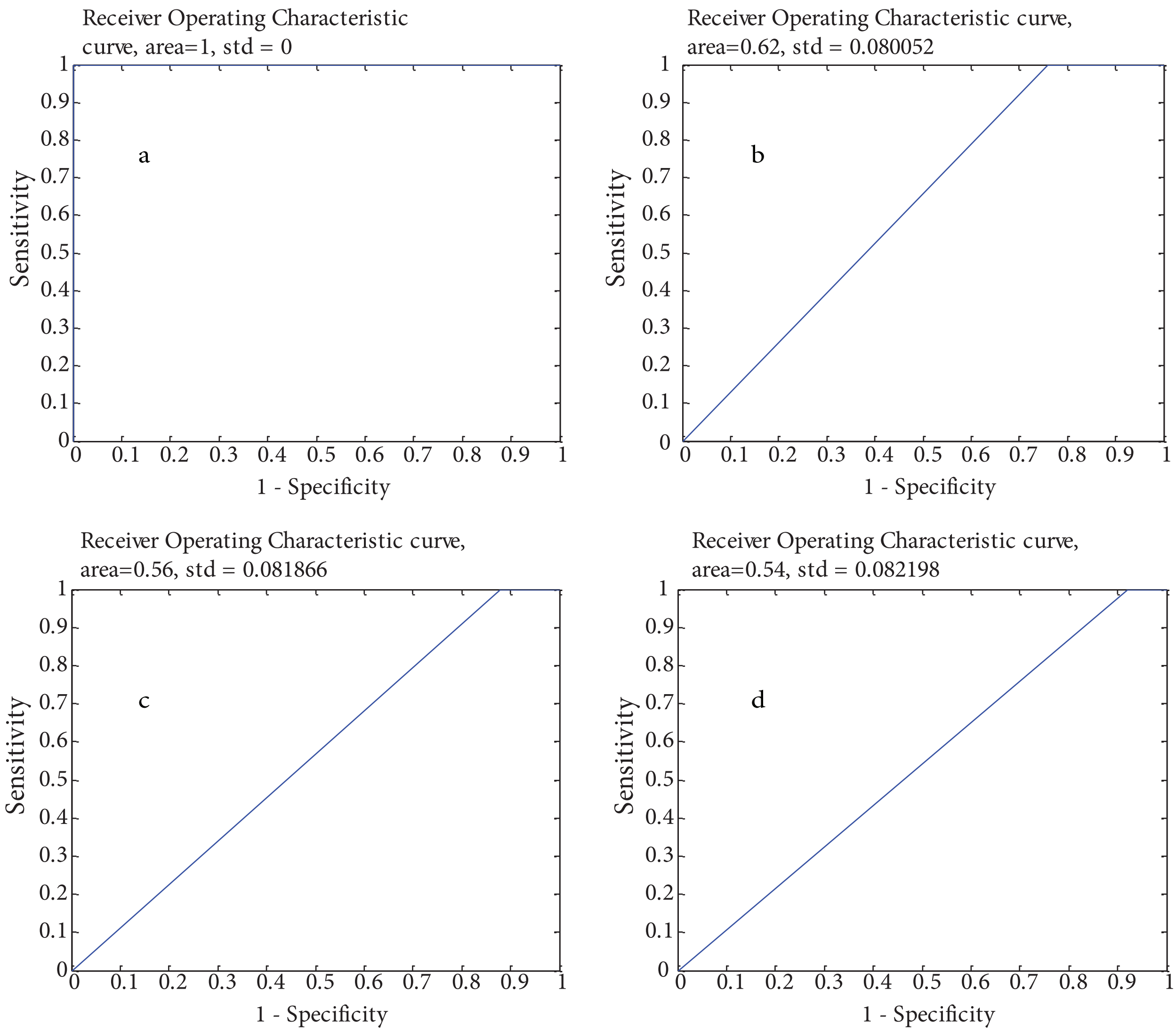


**Figure 4.** ROC curves for benign and malignant classification with wave atom coefficients. According to the values of sensitivity and specificity: a) for a scale of 1, b) for a scale of 2, c) for a scale of 3, and d) for a scale of 4.

**Table 3.** Success rates of the SVM algorithm in the classification of mammogram images as normal and abnormal after applying PCA.

| | | Wave atom + PCA | | | |
|---|---|---|---|---|---|
| Scale | PCA component | Accuracy (%) | Sensitivity | Specificity | Classifier |
| **1** | 2 | 98 | 0.98 | 1 | SVM |
| | 3 | 95 | 0.91 | 1 | |
| | 4 | 96 | 0.92 | 1 | |
| | 6 | 96 | 0.92 | 1 | |
| | 9 | 96 | 0.92 | 1 | |
| **2** | 2 | 93 | 0.87 | 1 | SVM |
| | 3 | 94 | 0.89 | 1 | |
| | 4 | 100 | 1 | 1 | |
| | 6 | 100 | 1 | 1 | |
| | 9 | 100 | 1 | 1 | |
| **3** | 2 | 95 | 0.91 | 1 | SVM |
| | 3 | 96 | 0.92 | 1 | |
| | 4 | 100 | 1 | 1 | |
| | 6 | 100 | 1 | 1 | |
| | 9 | 99 | 0.99 | 1 | |
| **4** | 2 | 83 | 0.66 | 1 | SVM |
| | 3 | 89 | 0.78 | 1 | |
| | 4 | 88 | 0.76 | 1 | |
| | 6 | 90 | 0.80 | 1 | |
| | 9 | 96 | 0.92 | 1 | |

**Table 4.** Success rates of the SVM algorithm in the classification of mammogram images as malignant and benign after applying PCA.

| | | Wave atom + PCA | | | |
|---|---|---|---|---|---|
| Scale | PCA component | Accuracy (%) | Sensitivity | Specificity | Classifier |
| **2** | 2 | 52 | 1 | 0.04 | SVM |
| | 3 | 52 | 0.53 | 0.51 | |
| | 4 | 52 | 0.53 | 0.51 | |
| | 6 | 60 | 0.77 | 0.43 | |
| | 9 | 80 | 0.80 | 0.80 | |
| **3** | 2 | 54 | 1 | 0.08 | SVM |
| | 3 | 62 | 1 | 0.24 | |
| | 4 | 60 | 1 | 0.20 | |
| | 6 | 62 | 0.61 | 0.57 | |
| | 9 | 92 | 0.88 | 0.95 | |
| **4** | 2 | 46 | 0.45 | 0.47 | SVM |
| | 3 | 64 | 1 | 0.28 | |
| | 4 | 56 | 0.63 | 0.49 | |
| | 6 | 50 | 0.50 | 0.50 | |
| | 9 | 52 | 0.53 | 0.51 | |

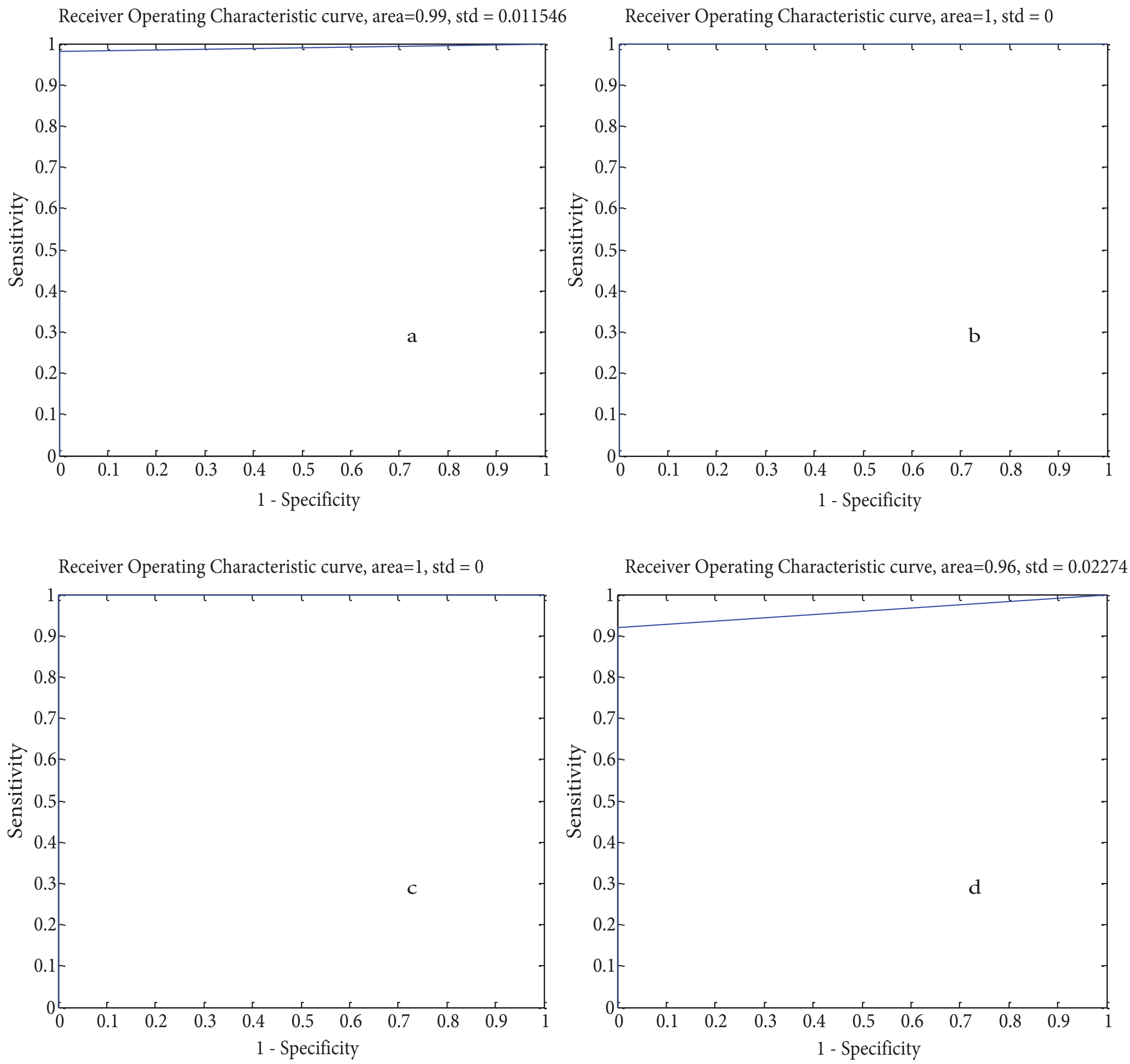


**Figure 5.** ROC curves for normal and abnormal classification with wave atom coefficients and PCA. According to the maximum values of sensitivity and specificity: a) for a scale of 1, b) for a scale of 2, c) for a scale of 3, and d) for a scale of 4.

## 5. Conclusion

Breast cancer diagnosis using a digital mammogram is a practical field of investigation of diseases for medical application. The positive results that come from CAD systems affect the mortality rate of patients. In the scope of the study, this paper describes a CAD system for recognizing breast cancer in ROIs of digital mammograms. The study also investigates the performance of the system with the WAT, PCA, and SVM methods. The best success rates in this work are obtained with coefficients at a scale of 1, 2, and 3 using SVM with PCA. The presented results demonstrate that WAT, PCA, and SVM are useful and powerful methods to distinguish the mammographic images as normal, benign, and malignant. We observed that using WAT and SVM provides

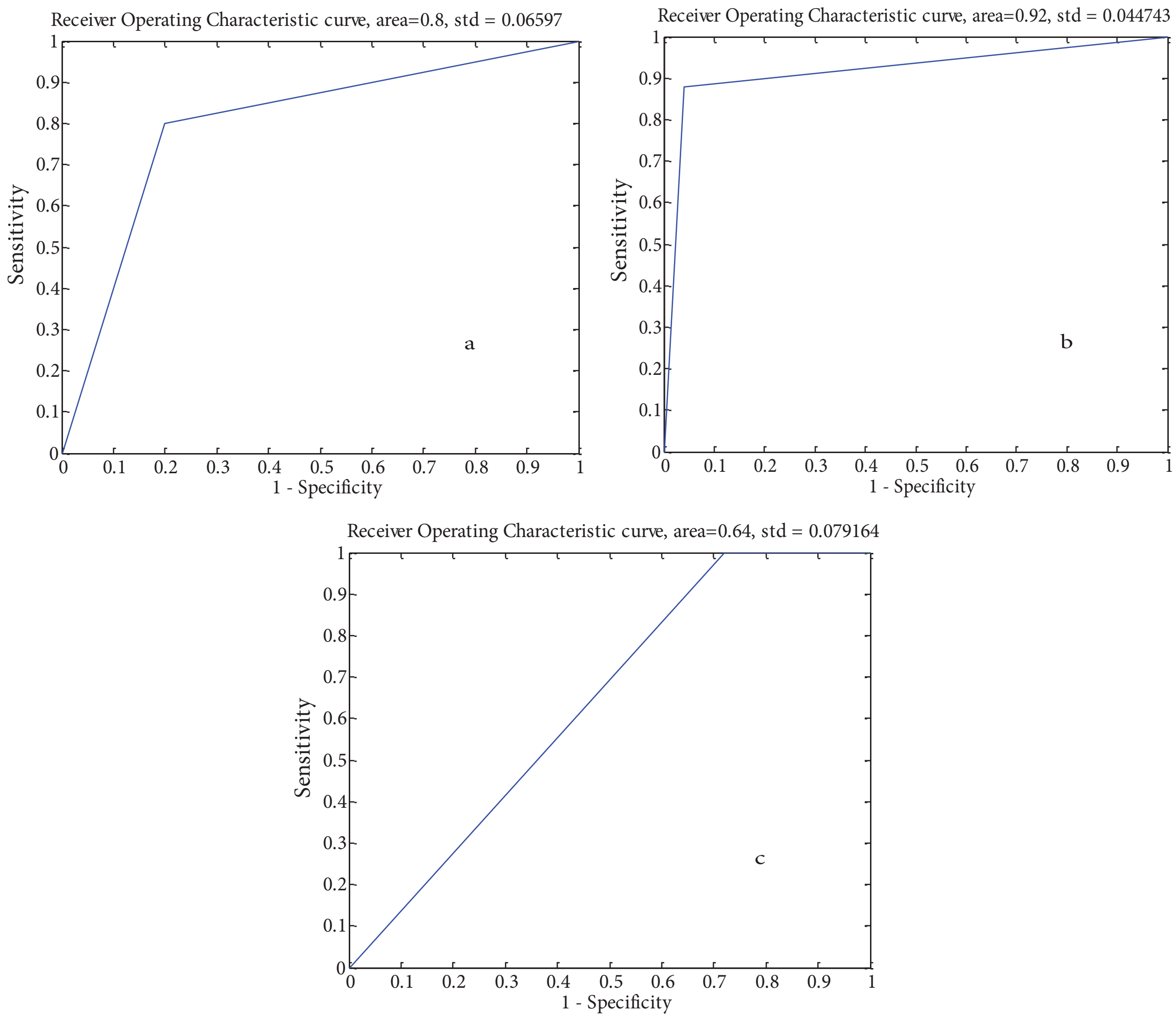


**Figure 6.** ROC curves for benign and malignant classification with wave atom coefficients and PCA. According to the maximum values of sensitivity and specificity: a) for a scale of 2, b) for a scale of 3, c) for a scale of 4.

great advantage for normal/abnormal classification. Using the WAT and SVM with PCA method, an accuracy rate of 100% is achieved for normal/abnormal classification. For malignant/benign classification, an accuracy rate of 100% is also achieved using the WAT and SVM methods. From these results, it is observed that such features provide important support for more detailed clinical investigations and the results are very encouraging when mammograms are classified with WAT, PCA, and SVM.

## References

[1] N.R. Pal, B. Bhowmick, S.K. Patel, S. Pal, J. Das, "A multi-stage neural network aided system for detection of micro-calcifications in digitized mammograms", Neurocomputing, Vol. 71, pp. 2625–2634, 2008.

[2] J.C. Fu, S.K. Lee, S.T.C. Wong, J.Y. Yeh, A.H. Wang, H.K. Wu, "Image segmentation, feature selection and pattern classification for mammographic microcalcifications", Computerized Medical Imaging and Graphics, Vol. 29, pp. 419–29, 2005.

[3] R.M. Rangayyan, F.J. Ayres, J.E.L. Desautels, "A review of computer aided diagnosis of breast cancer: toward the detection of subtle signs", Journal of the Franklin Institute, Vol. 344, pp. 312–348, 2007.

[4] M.L. Giger, N. Krassemeijer, S.G. Armato, "Computer aided diagnosis in medical imaging", IEEE Transactions on Medical Imaging, Vol. 20, pp. 1205–1208, 2001.

[5] R.J. Ferrari, R.M. Rangayyan, J.E.L. Desautels, A.F. Frere, "Analysis of asymmetry in mammograms via directional filtering with Gabor wavelets", IEEE Transactions on Medical Imaging, Vol. 20, pp. 953–964, 2001.

[6] L. Bocchi, G. Coppini, J. Nori, G. Valli, "Detection of single and clustered microcalcifications in mammograms using fractals models and neural networks", Medical Engineering & Physics, Vol. 26, pp. 303–312, 2004.

[7] I. Christoyianni, A. Koutras, E. Dermatas, G. Kokkinakis, "Computer aided diagnosis of breast cancer in digitized mammograms", Computerized Medical Imaging and Graphics, Vol. 26, pp. 309–319, 2002.

[8] L.F.A. Campos, A.C. Silva, A.K. Barros, "Diagnosis of breast cancer in digital mammograms using independent component analysis and neural networks", Proceedings of the 10th Iberoamerican Congress on Progress in Pattern Recognition, Image Analysis and Applications, Vol. 3773, pp. 460–469, 2005.

[9] D.D. Costa, L.F.A. Campos, A.K. Barros, "Classification of breast tissue in mammograms using efficient coding", Biomedical Engineering on Line, Vol. 10, pp. 50, 2011.

[10] C.Y. Wang, C.G. Wu, Y.C. Liang, X.C. Guo, "Diagnosis of breast cancer tumor based on ICA and LS-SVM", Proceedings of the 5th International Conference on Machine Learning and Cybernetics, pp. 2565–2570, 2006.

[11] K. Polat, S. Güneş, "Breast cancer diagnosis using least square support vector machine", Digital Signal Processing, Vol. 17, pp. 694–701, 2007.

[12] S.G. Mallat, "A theory for multiresolution signal decomposition: the wavelet representation", IEEE Transactions on Pattern Analysis and Machine Intelligence, Vol. 7, pp. 674–693, 1989.

[13] R. Mousa, Q. Munib, A. Moussa, "Breast cancer diagnosis system based on wavelet analysis and fuzzy-neural", Expert Systems with Applications, Vol. 28, pp. 713–723, 2005.

[14] K.K. Rajkumar, G. Raju, "A comparative study on classification of mammogram images using different wavelet transformations", International Journal of Machine Intelligence, Vol. 3, pp. 310–317, 2011.

[15] G. Boccignone, A. Chianese, A. Picariello, "Computer aided detection of microcalcifications in digital mammograms", Computers in Biology and Medicine, Vol. 30, pp. 267–286, 2000.

[16] M.N. Gurcan, Y. Yardımcı, A.E. Çetin, R. Ansari, "Automated detection and enhancement of microcalcifications in mammograms using nonlinear subband decomposition", Proceedings of the IEEE International Conference on Acoustics, Speech, and Signal Processing, Vol. 4, pp. 3069, 1997.

[17] M.N. Gurcan, Y. Yardımcı, A.E. Çetin, R. Ansari, "Detection of microcalcifications in mammograms using higher order statistics", IEEE Signal Processing Letters, Vol. 4, pp. 213–216, 1997.

[18] A.M. Bagci, A.E. Cetin, "Detection of microcalcifications in mammograms using local maxima and adaptive wavelet transform analysis", IEEE Electronics Letters, Vol. 38, pp. 1311–1313, 2002.

[19] F. Moayedi, Z. Azimifar, R. Boostani, S. Katebi, "Contourlet-based mammography mass classification", Lecture Notes in Computer Science, Vol. 4633, pp. 923–934, 2007.

[20] E.J. Candès, D.L. Donoho, "Curvelets, multiresolution representation, and scaling laws", SPIE Wavelet Applications in Signal and Image Processing VIII, Vol. 4119, 2000.

[21] F.E. Ali, I.M. El-Dokany, A.A. Saad, F.E. Abd El-Samie, "Curvelet fusion of MR and CT images", Progress in Electromagnetics Research, Vol. 3, pp. 215–224, 2008.

[22] N.T. Binh, N.C. Thanh, "Object detection of speckle image base on curvelet transform", ARPN Journal of Engineering and Applied Sciences, Vol. 2, pp. 14–16, 2007.

[23] M.M. Eltoukhy, I. Faye, B.B. Samir, "A comparison of wavelet and curvelet for breast cancer diagnosis in digital mammogram", Computers in Biology and Medicine, Vol. 40, pp. 384–391, 2010.

[24] M.M. Eltoukhy, I. Faye, B.B. Samir, "Breast cancer diagnosis in digital mammogram using multiscale curvelet transform", Computerized Medical Imaging and Graphics, Vol. 34, pp. 269–276, 2010.

[25] M.M. Eltoukhy, I. Faye, B.B. Samir, "A statistical based feature extraction method for breast cancer diagnosis in digital mammogram using multiresolution representation", Computers in Biology and Medicine, Vol. 42, pp. 123–128, 2012.

[26] L. Demanet, L.X. Ying, "Wave atoms and sparsity of oscillatory patterns", Applied and Computational Harmonic Analysis, Vol. 23, pp. 368–387, 2007.

[27] Mammographic Image Analysis Society Database Web Page, 2012. Available at: http://peipa.essex.ac.uk/info/mias.html.